

CONF-8905184--1  
CONF-890730-Received by OSTI

**DISCLAIMER**

JUL 1 0 1989

This report was prepared as an account of work sponsored by an agency of the United States Government. Neither the United States Government nor any agency thereof, nor any of their employees, makes any warranty, express or implied, or assumes any legal liability or responsibility for the accuracy, completeness, or usefulness of any information, apparatus, product, or process disclosed, or represents that its use would not infringe privately owned rights. Reference herein to any specific commercial product, process, or service by trade name, trademark, manufacturer, or otherwise does not necessarily constitute or imply its endorsement, recommendation, or favoring by the United States Government or any agency thereof. The views and opinions of authors expressed herein do not necessarily state or reflect those of the United States Government or any agency thereof.

CONF-8905184--1  
DE89 014093

## **Air Breakdown in the Relativistic Limit<sup>†</sup>**

Gerald Graham  
EG&G Energy Measurements, Inc.  
Los Alamos Operations  
P.O. Box 809, Los Alamos, NM 87544

R. Roussel-Dupré  
Los Alamos National Laboratory  
P.O. Box 1663, Los Alamos, NM 87545

<sup>†</sup>This work was supported by DOE Contract No. DE-AC08-88NV10617.

MASTER

sb  
DISTRIBUTION OF THIS DOCUMENT IS UNLIMITED

## **DISCLAIMER**

**This report was prepared as an account of work sponsored by an agency of the United States Government. Neither the United States Government nor any agency thereof, nor any of their employees, makes any warranty, express or implied, or assumes any legal liability or responsibility for the accuracy, completeness, or usefulness of any information, apparatus, product, or process disclosed, or represents that its use would not infringe privately owned rights. Reference herein to any specific commercial product, process, or service by trade name, trademark, manufacturer, or otherwise does not necessarily constitute or imply its endorsement, recommendation, or favoring by the United States Government or any agency thereof. The views and opinions of authors expressed herein do not necessarily state or reflect those of the United States Government or any agency thereof.**

---

## **DISCLAIMER**

**Portions of this document may be illegible in electronic image products. Images are produced from the best available original document.**

# Introduction

RELF LAP, a relativistic fluid code for high-power microwave propagation through the atmosphere, has been applied to the study of electrical breakdown of air. This code was used to extend the benchmark curve of  $E/P$  vs.  $P\tau$  to the relativistic regime. The lack of a collisional relativistic code has limited the range of this curve in the past.

RELF LAP solves the relativistic fluid equations and the Maxwell equations for the temporal behavior of the fields as a microwave propagates through the atmosphere. Electron densities, momenta, and thermal energies are also calculated by the code. Relativistic expressions for the effective dc electric field of a microwave pulse and the formative time for air breakdown are derived. These expressions are confirmed by plotting microwave breakdown curves of different frequencies on the same  $E_{eff}/P$  vs.  $P\tau$  curve. The new scaling of the problem in terms of  $E_{eff}/\nu$  vs.  $\nu\tau$  is also applied to the relativistic regime.

The ponderomotive force is included in this relativistic model. The effects of this force on formative times for air breakdown and on electron density, momentum, and thermal energy are discussed here. The nonrelativistic results of our code were compared with the experimental data of Felsenthal and Proud,<sup>1</sup> and Yee et al.,<sup>2</sup> and with the fluid code of Roussel-Dupré et al.<sup>3</sup> These comparisons show excellent agreement over the

entire range. Although experimental data in the relativistic regime are not available, pulse trajectories from some experiments have shown a shift of breakdown from the leading edge of the pulse to the trailing edge.<sup>4</sup> This shift is associated with the turning of the breakdown curve at  $E/P \approx 10^4$  volts/cm/Torr and occurs at the beginning of the relativistic regime.

# Theory

## Fluid Equations

The relativistic fluid equations in retarded time at a fixed position are:

$$\frac{\partial n_e(1 - \beta_{ox})}{\partial \tau} = R_c n_e \quad (1)$$

$$(1 - \beta_{ox}) \frac{\partial p_x}{\partial \tau} - \frac{2}{n_e 3mc^2} \frac{\partial}{\partial \tau} \frac{n_e T'}{\gamma_o} + \frac{e}{mc} [E_{cs} + \beta_{ox} B] = - (R_m + R_c) p_x \quad (2)$$

$$(1 - \beta_{ox}) \frac{\partial p_z}{\partial \tau} + \frac{e}{mc} [E_o - \beta_{ox} B] = - (R_m + R_c) p_z \quad (3)$$

$$(1 - \beta_{ox}) \frac{\partial T'}{\partial \tau} = (R_E - R_c) T' \quad (4)$$

- $R_c$ ,  $R_m$ , and  $R_E$  are the particle, momentum, and energy exchange rates.
- $\beta_{ox}$  is the mean electron velocity in the direction of microwave propagation.
- $\beta_{oz}$  is the mean electron velocity in the direction of the applied electric field.

The approximate Maxwell equations that were used in RELFLAP for the electric and magnetic fields are:

$$\frac{\partial E_{cs}}{\partial \tau} = 4\pi e c n_e \beta_{ox} \quad (5)$$

$$\frac{\partial B}{\partial \tau} = 4\pi e c n_e \beta_{ox} + \frac{\partial E_o}{\partial \tau} \quad (6)$$

$$\frac{\partial E_o}{\partial x} = -\frac{2\pi}{c} e c n_e \beta_{ox} \quad (7)$$

- $\vec{E}_o$  and  $\vec{B}$  are the applied electric and magnetic fields, respectively.
- $E_{cs}$  is the charge separation electric field.

$$P\tau$$

The relativistic expression for the formative time for air breakdown is found to be

$$P\tau = \frac{P(1 - \beta_{ox})}{R_c} \ln \left[ \frac{n_e(1 - \beta_{ox})}{n_o} \right] \quad (8)$$

- $n_o$  is the initial electron density of the air.
- The nonrelativistic expression for  $p\tau$  is obtained by taking the limit  $\beta_{ox} \rightarrow 0$ .

## Relativistic Effective Field

- Results in the same ionization rate that the microwave electric field produces.
- Enables comparison of the dc breakdown curve with microwave breakdown curves.
- Produces the same electron momentum in the direction of the applied field,  $p_z$ .

### The DC-Field Case

For the case when  $E_o$  is constant, the equivalent root-mean-square value of  $p_z$  becomes

$$p_{z,rms} = \frac{e}{mc} \frac{E_o}{\nu} \quad (9)$$

where  $\nu = (R_m + R_c)/(1 - \beta_{ox})$ .

### Microwave Case

For the case when  $E_o = E_{op} \sin \omega \tau$ , we find the root-mean-square of the momentum  $p_z$  to be

$$p_{z,rms}^{\mu} = \frac{e}{mc} \frac{E_{op}}{\sqrt{2}} \frac{1}{\nu \sqrt{1 + \omega^2/\nu^2}} \quad (10)$$

By comparing Eq. 9 to Eq. 10, we find the relativistic effective field to be

$$E_{eff} = \frac{E_{rms}}{\sqrt{1 + \omega^2/\nu^2}}$$

where  $\nu$  is the weighted collision frequency for momentum transfer  $(R_m + R_c)/(1 - \beta_{ox})$ .

- The relativistic expressions for  $P\tau$  and  $E_{eff}$  are used in Figure 1 to plot air breakdown thresholds.

$E/\nu$  vs.  $\nu\tau$

- The  $E_{eff}/P$  vs.  $P\tau$  scaling of the air breakdown problem depended on an approximate expression for the momentum exchange rate; namely,  $\nu = 5.3(10^9)P$ .
- $E/\nu$  vs.  $\nu\tau$  is the correct scaling law that was derived for an energy dependent  $\nu$ .<sup>3</sup>
- To obtain the relativistic equivalent of this new scaling law, let  $\nu = (R_m + R_c)/(1 - \beta_{ox})$ .
- Figure 2 confirms that a curve of  $E_{eff}/\nu$  vs.  $\nu\tau$  is a better scaling law for air breakdown thresholds.

# Results

When an applied electric field is very strong, electrons are accelerated to relativistic speeds. The fast electrons that were accelerated by a microwave electric field are pushed into the direction of propagation by the ponderomotive force, namely  $\vec{\beta} \times \vec{B}$  in this case. For a dc electric field the ponderomotive force is absent and the electron velocity  $\beta_{ox}$  is zero. For microwave fields, electrons are initially pulled along with the propagating pulse, resulting in some interesting effects on electron density, momentum, and energy. These effects are reflected in the  $(1 - \beta_{ox})$  terms that appear in the earlier equations.

## Air Breakdown in the Relativistic Regime

### Density

- The electron density is enhanced by the electrons that are pulled along with the microwave pulse.
- This enhancement occurs in two separate ways.
  1. The initial electron density is effectively increased when the “original” free electrons are pulled along with the pulse. This density increase is represented by  $n_o/(1 - \beta_{ox})$ , where  $n_o$  is the initial electron energy.

2. Free electrons that are produced through ionization are also pulled along with the pulse resulting in an effective ionization rate  $R_c/(1 - \beta_{ox})$ .

### Formative Time

- The density enhancement leads to shorter formative times for air breakdown.
- In Figure 1 this effect can be seen as the microwave curves splitting away from the dc curve for  $E_{eff}/P \geq 2(10^4)$  volts/cm/Torr.
- Nonrelativistic theory of air breakdown predicts no differences in densities or breakdown times between microwave and dc pulses with the same effective electric field.

### Electron Velocity

- The electron velocity  $\beta_{ox}$  can be easily calculated from experimental data because of the differences between formative times for dc pulse and microwave pulse air breakdown in the relativistic regime.

$$\beta_{ox} \approx 1 - \frac{P\tau_\mu}{P\tau_{dc}} \quad (11)$$

- The electron velocity  $\beta_{ox}$  can be calculated from experimental data using Eq. 11 if one uses Figure 1 to estimate a value for  $P\tau_{dc}$ .

## Relativistic Regime

- The plot of  $E_{eff}/P$  vs.  $P\tau$  in Figure 1 shows that the curve turns back toward lower values of  $P\tau$  in the relativistic regime.
- This turning back of the curve is due to the behavior of the ionization rate at high electron energies.<sup>3</sup>
- The behavior of the ionization rate, shown in a plot of  $\nu_i/P$  vs.  $E_{eff}/P$  in Figure 3, is mimicked by the plot of  $E_{eff}/P$  vs.  $P\tau$  in Figure 1.

## Experiments

- Results from our relativistic code for nonrelativistic energies were compared with the results of the nonrelativistic fluid code of Roussel-Dupré et al.<sup>3</sup> and with the experimental data of Felsenthal and Proud,<sup>1</sup> and Yee et al.<sup>2</sup> (Figure 4).
- The approximation  $\nu = 5.3(10^9)P$  used in computing effective fields for microwave data underestimates the collision frequency for most values of  $E/P$  above 50 volts/cm/Torr (Figure 5).
- An energy dependent collision frequency would adjust microwave data closer to our relativistic curve.
- Experimental data in the relativistic regime are not yet available.

## Momentum

- In the absence of the ponderomotive force, the mean electron momentum in this problem is the momentum in the direction of the applied electric field,  $p_z$ .
- The ponderomotive force pushes the mean momentum in the direction of propagation, but does not reduce its magnitude.
- The electron momentum  $p_z$  is reduced while the electron momentum  $p_x$  is increased.
- The changes in the electron momentum are represented in the effective momentum collision frequency  $\nu = \frac{R_m + R_c}{(1 - \beta_{ox})}$ .
- The plot of  $p_z$  vs.  $E_{eff}/\nu$  in Figure 6 clearly shows the lower momentum  $p_z$  in the relativistic regime for microwave pulses.
- Figure 7 confirms that the total mean momentum remains unchanged.

## Energy

- Since the magnitude of the momentum for microwave induced air breakdown remains unchanged from the momentum for dc breakdown, the kinetic energy will also be unchanged.
- The increase in the collision frequency that occurs when electrons are pulled along with a microwave pulse leads to greater energy loss from the pulse and increases the mean electron thermal energy of the breakdown region.
- At a fixed position

$$T' = T'_o e^{\frac{(R_E - R_c)}{(1 - \beta_{ox})} \tau}$$

where  $T'_o$  is the initial electron thermal energy.

- The effective energy exchange rate  $\frac{R_E - R_c}{(1 - \beta_{ox})}$  suggests the increase in electron thermal energy for microwave induced breakdown.
- This higher thermal energy associated with microwave pulse breakdown is clearly seen in the plot of thermal energy vs.  $E_{eff}/\nu$  in Figure 8.

## Summary

RELF LAP, the relativistic fluid code for high-power microwave propagation, has been applied to the calculation of the  $E/P$  vs.  $P\tau$  curve for breakdown in air. Previous calculations of the  $E/P$  vs.  $P\tau$  curve were stopped when  $P\tau$  reached a value of  $4 \times 10^{-9}$  Torr sec. Our relativistic calculation has confirmed that the curve turns back toward lower values of  $P\tau$  beyond this point. This phenomena is due to the behavior of the ionization rate at high electron energies.

Relativistic expressions for the formative time for air breakdown and the effective dc electric field of a microwave pulse were derived. These expressions were confirmed by plotting microwave breakdown curves of different frequencies on the same curve. The energy dependence of the momentum exchange frequency leads to the relativistic extension of the scaling law for air breakdown thresholds. Microwave and dc pulse breakdown thresholds lie together along this entire  $E_{eff}/\nu$  vs.  $\nu\tau$  curve.

Electrons that are initially pulled along with a microwave pulse due to the ponderomotive force, lead to earlier breakdown times. This is seen by the splitting of the  $E/P$  vs.  $P\tau$  curve between microwave and dc results in Figure 1. The ponderomotive electrons also lead to enhanced electron densities and thermal energies and reduced electron momentum in the direction of the applied field.

The nonrelativistic results of our code were compared with the experimental data of Felsenthal and Proud, and Yee et al., and with the fluid code of Roussel-Dupré et al. These comparisons show good agreement over most of the nonrelativistic region. Experimental data in the relativistic regime are not available.

## Figures

FIG. 1. Air breakdown thresholds in terms of  $E_{eff}/P$  vs.  $P\tau$  for dc-pulse breakdown and 1-GHz, 5-GHz, and 10-GHz microwave pulse breakdown. An energy dependent momentum exchange frequency was used to calculate  $E_{eff}$ . Relativistic effects are first seen above  $E_{eff}/P = 2(10^4)$  volts/cm/Torr.

FIG. 2. Air breakdown thresholds in terms of  $E_{eff}/\nu$  vs.  $\nu\tau$  for dc and microwave pulse breakdown.

FIG. 3. The maximum in the ionization rate  $\nu_i$  corresponds to the minimum in the formative time for air breakdown. The behavior of the ionization rate as it turns back up at higher electron energy is mimicked in the plot of  $E_{eff}/P$  vs.  $P\tau$ .

FIG. 4. The Felsenthal and Proud data plotted here are for dc-pulse breakdown, while the data of Yee et al. are for 2.586-GHz microwave pulse breakdown. An energy dependent collision frequency would adjust the microwave data closer to our relativistic curve.

FIG. 5. The approximation  $\nu = 5.3(10^9)P$  underestimates the collision frequency for  $E_{eff}/P > 40$  volts/cm/Torr.

FIG. 6. For microwave pulse breakdown, the ponderomotive force reduces the electron momentum  $p_z$  and increases the momentum  $p_x$ . This effect is not present in dc-pulse breakdown.

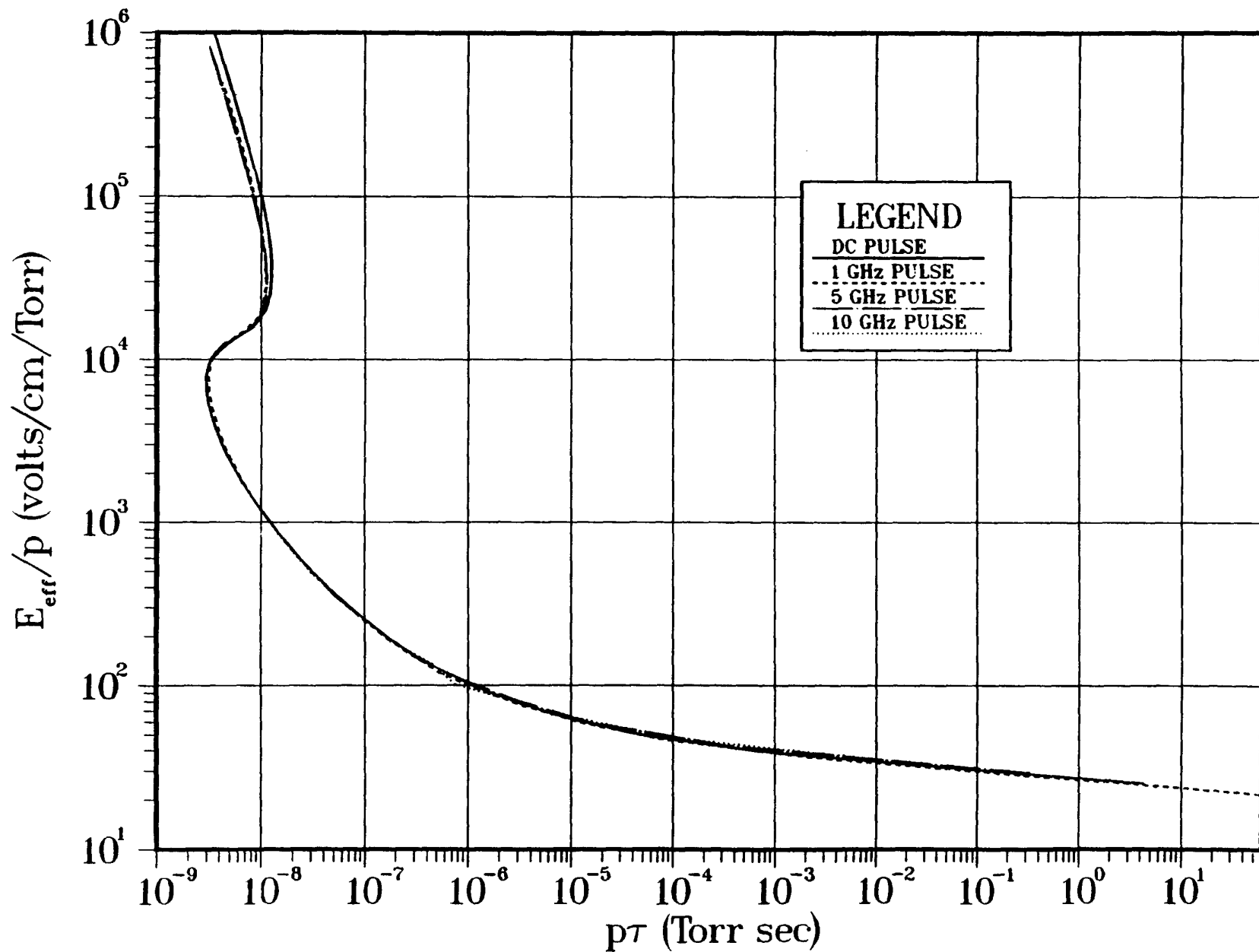
FIG. 7. No differences exist between the dc and microwave curves for total mean electron momentum.

FIG. 8. The mean electron thermal energy is enhanced by the effect of the ponderomotive force.

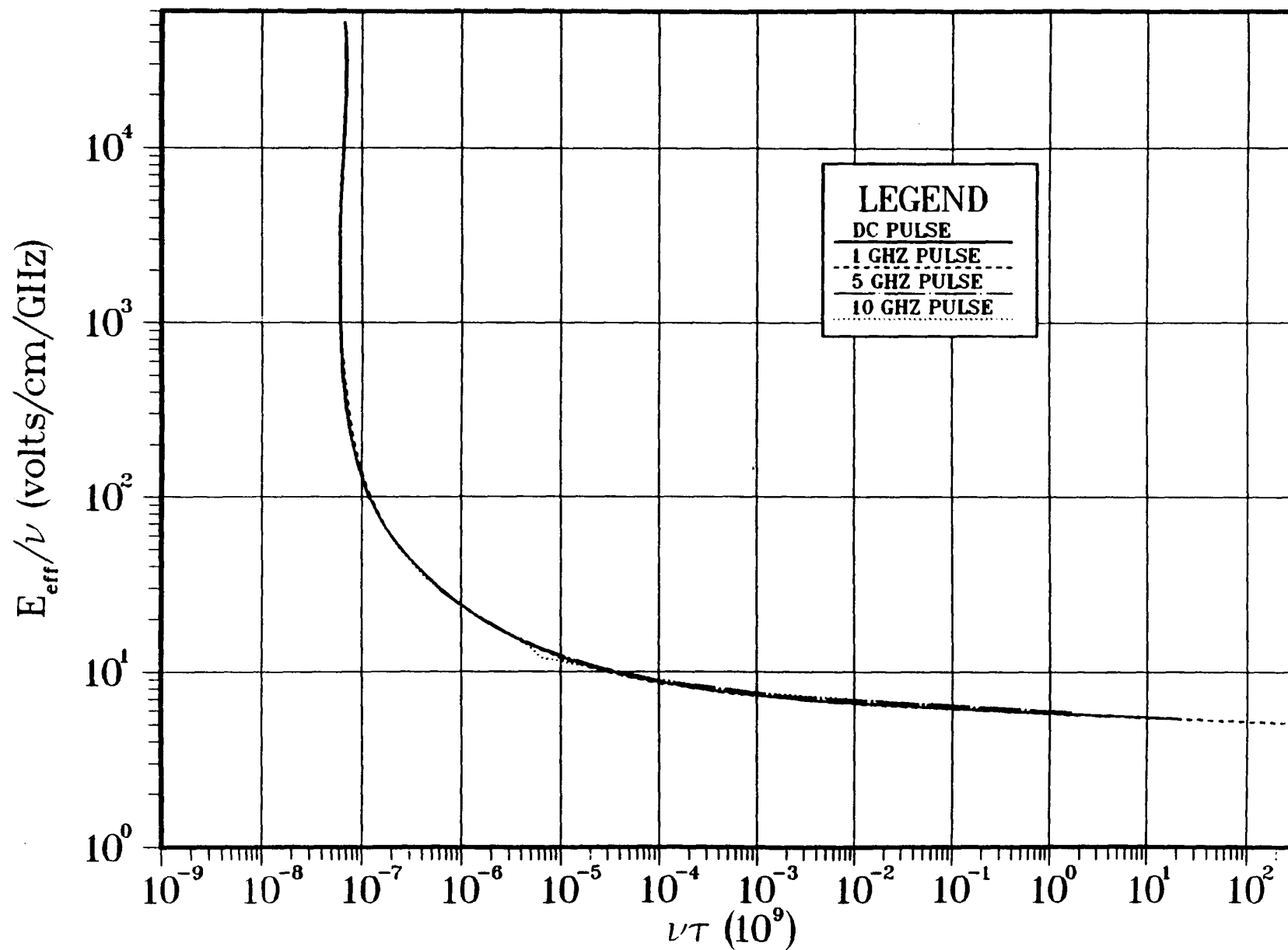
## References

- <sup>1</sup>P. Felsenthal and J. M. Proud, Phys. Rev. **139**, A1796 (1965).
- <sup>2</sup>J. H. Yee, R. A. Alvarez, D. J. Mayhall, D. P. Byrne, and J. DeGroot, Phys. Fluids **29**, 1238 (1986).
- <sup>3</sup>R. A. Roussel-Dupré et al., High-power microwave propagation in air, Fourth National Conference on High Power Microwave Technology, Naval Post Graduate School, Monterey, CA, May 1988.
- <sup>4</sup>R. A. Alvarez, private communication.

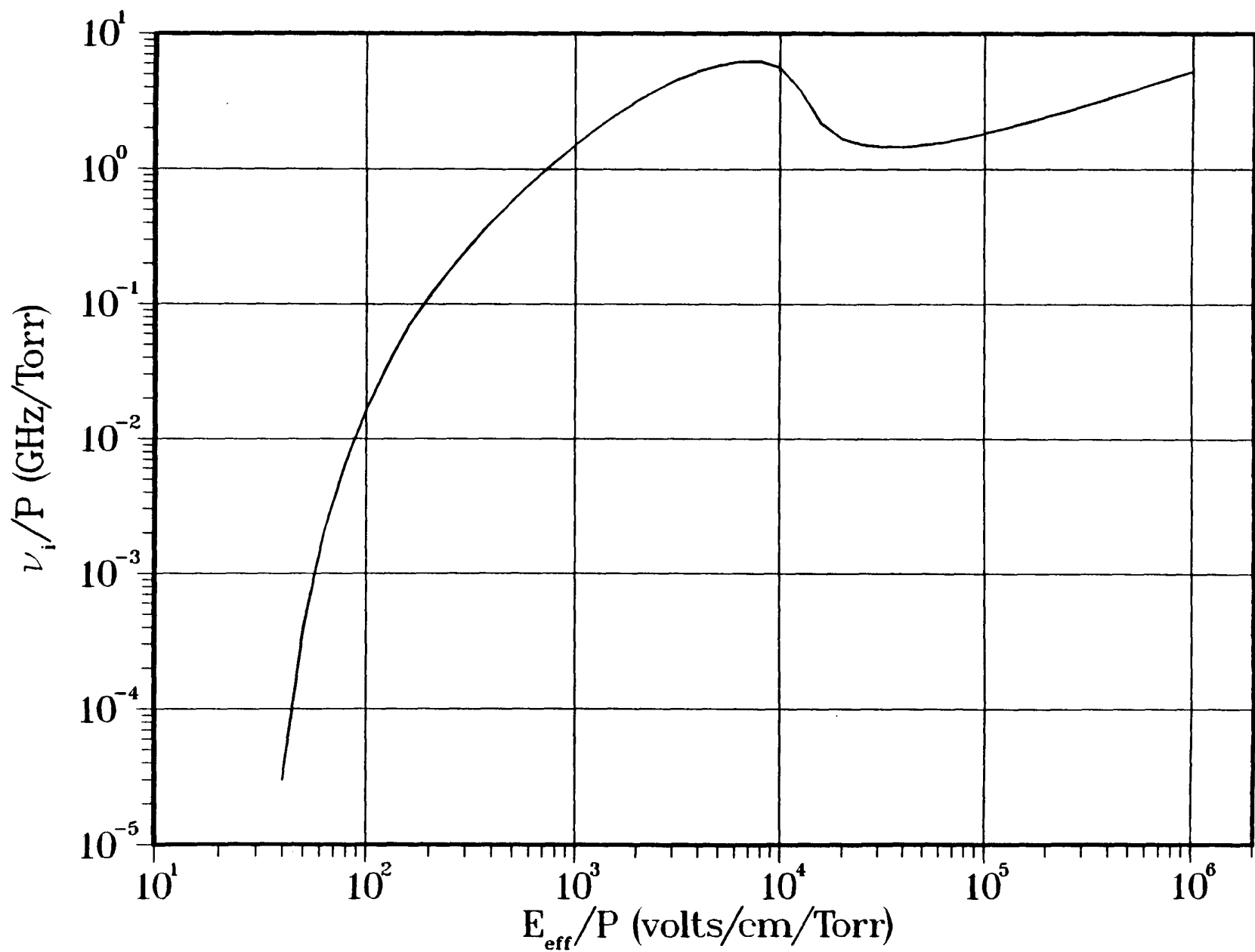
# Air Breakdown Threshold



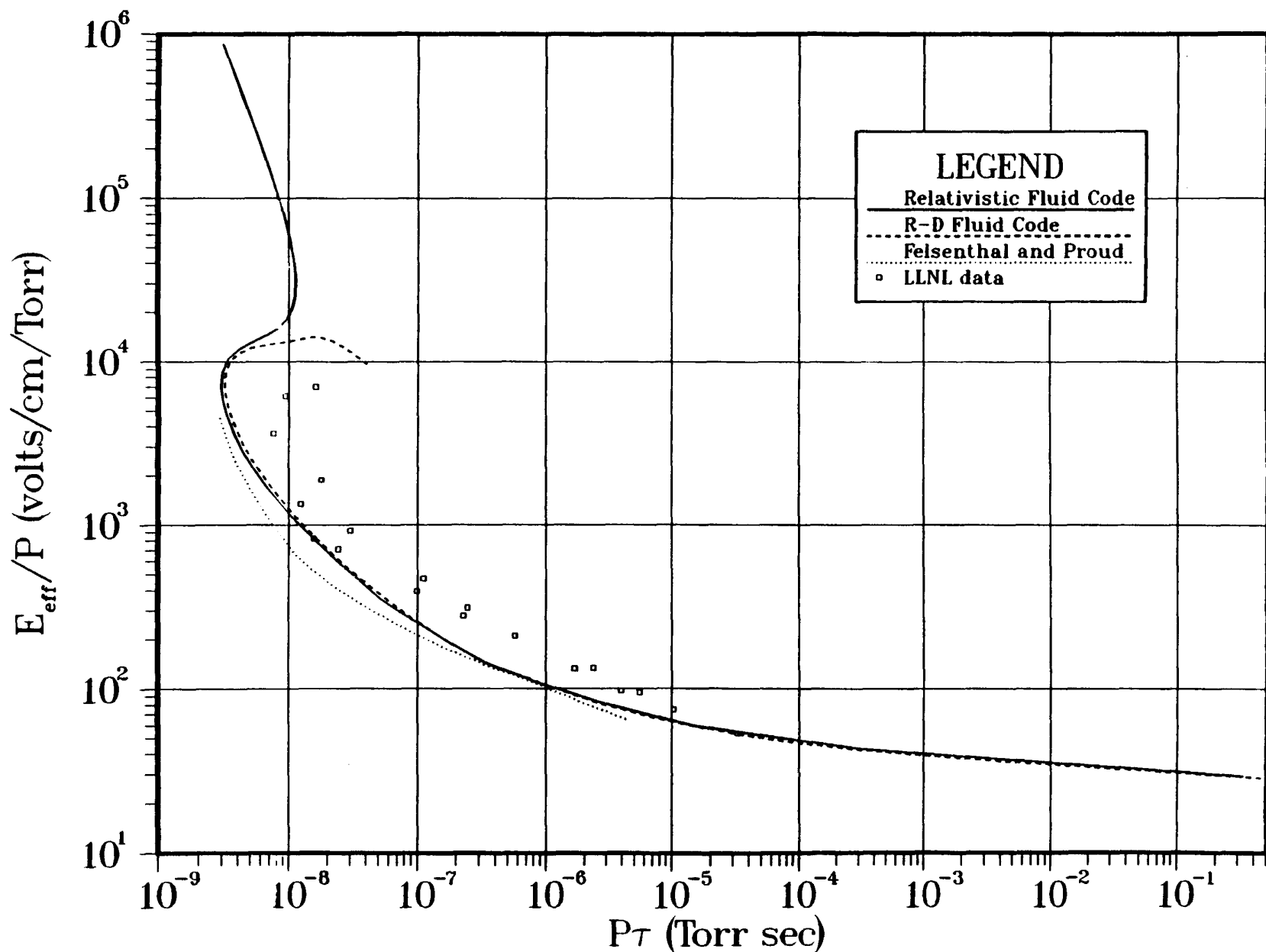
# Air Breakdown Threshold



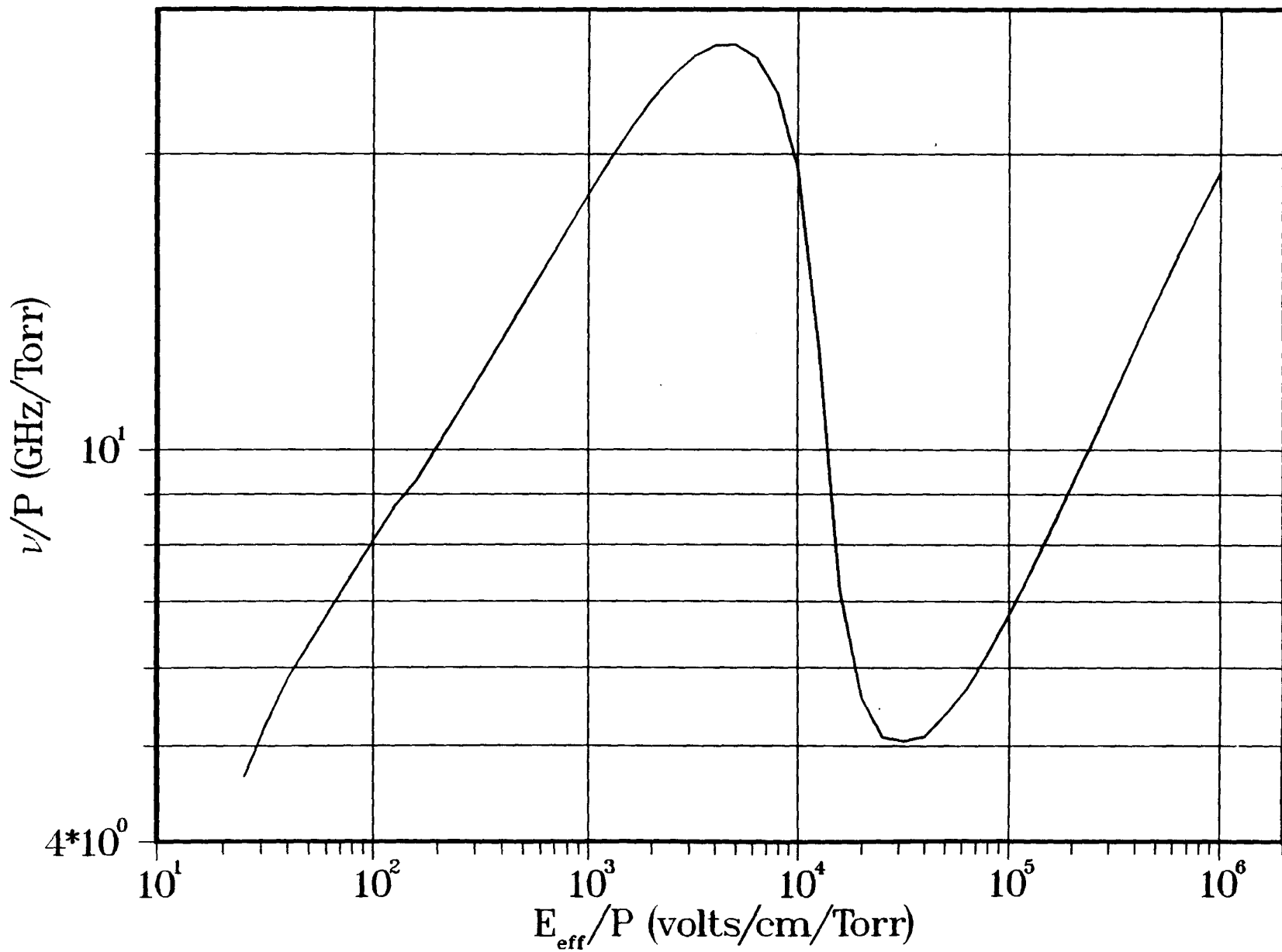
$\nu_i/P$  vs.  $E_{\text{eff}}/P$



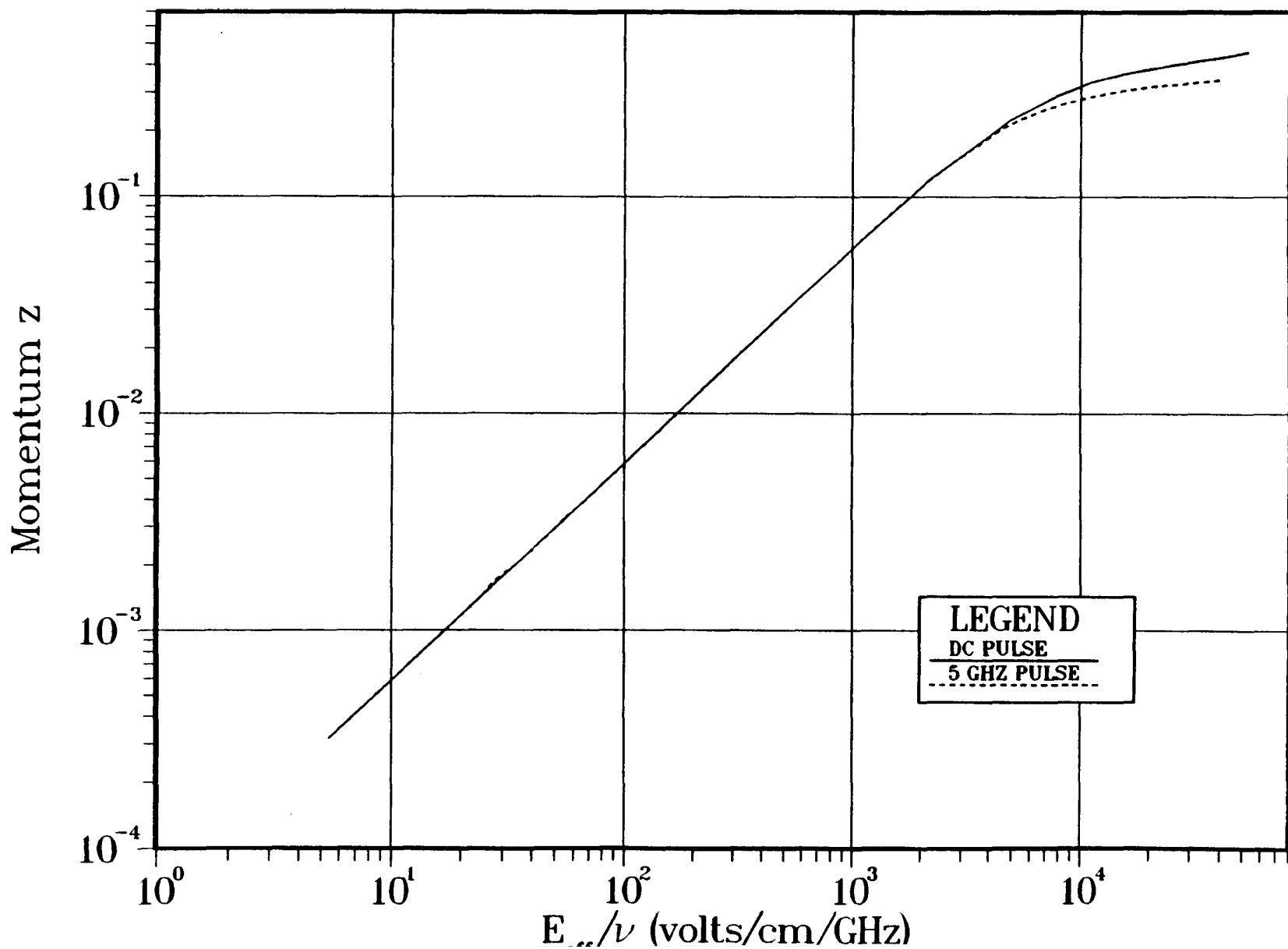
# Air Breakdown Threshold



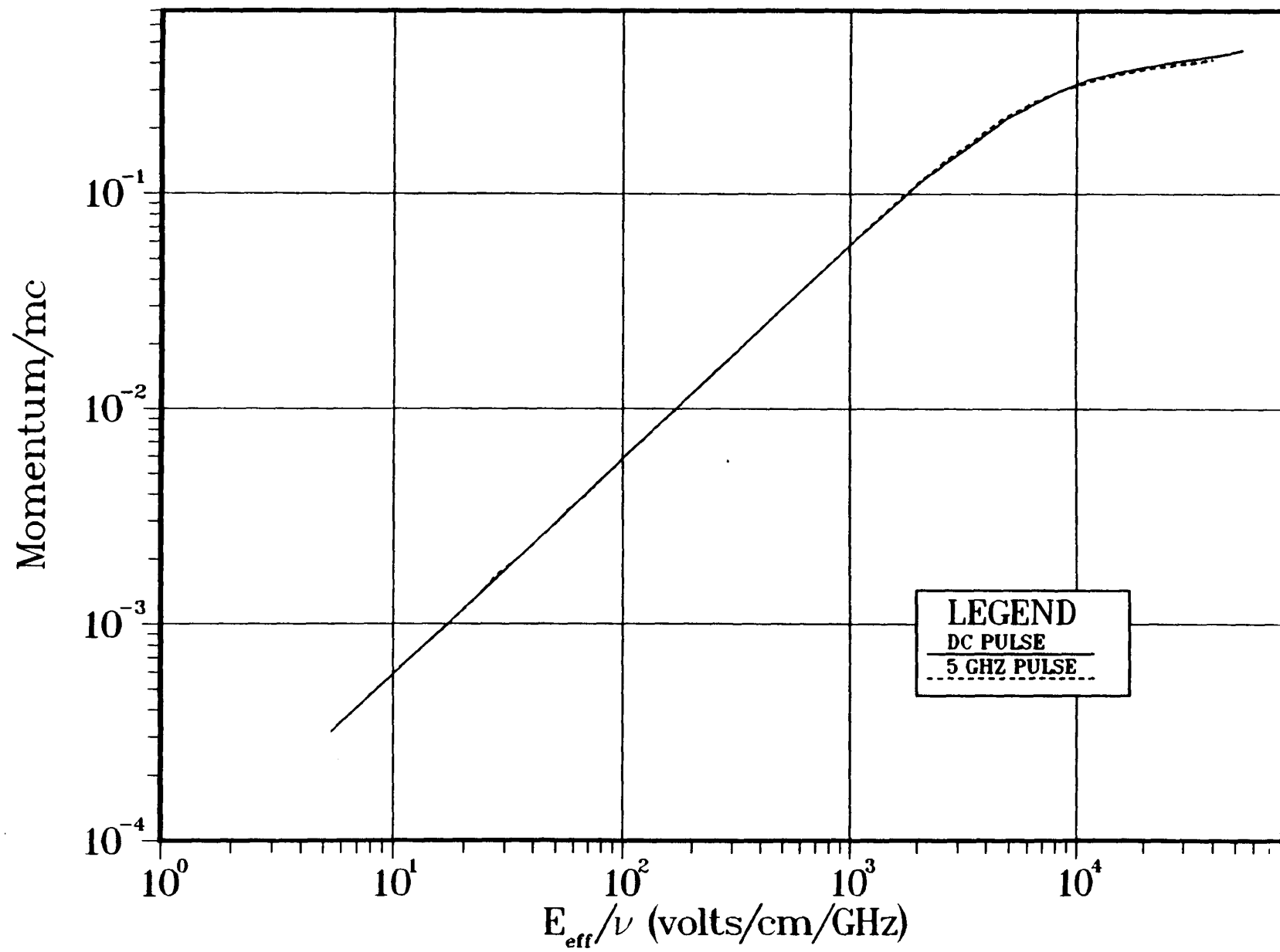
## Collision Frequency vs. $E_{\text{eff}}/P$



# Momentum z vs. $E_{\text{eff}}/\nu$



# Momentum/mc vs. $E_{\text{eff}}/\nu$



# Thermal Energy vs. $E_{\text{eff}}/\nu$

